Toroidal Flux Oscillations as Possible Causes of Geomagnetic Excursions and Reversals

F. H. Busse

Institute of Physics, University of Bayreuth, D-95440 Bayreuth, Germany

R. D. Simitev

Department of Mathematics, University of Glasgow, G12 8QW Glasgow, UK

Abstract

It is proposed that convection driven dynamos operating in planetary cores could be oscillatory even when the oscillations are not directly noticeable from the outside. Examples of dynamo simulations are pointed out that exhibit oscillations in the structure of the azimuthally averaged toroidal magnetic flux while the mean poloidal field shows only variations in its amplitude. In the case of the geomagnetic field, global excursions may be associated with these oscillations. Long period dynamo simulations indicate that the oscillations may cause reversals once in a while. No special attempt has been made to use most realistic parameter values. Nevertheless some similarities between the simulations and the paleomagnetic record can be pointed out.

Key words: geodynamo, excursions, reversal, dynamo oscillations

1 Introduction

The origin of geomagnetic reversals is a much debated subject among scientists in the fields of paleomagnetism and dynamo theory. There is general agreement that a detailed understanding of reversals is a key issue of geodynamo theory. In this connection also the problem of global excursions of the geomagnetic field in which the dipole strength reaches temporarily unusually low values has been discussed and it has been suggested (*Doell & Cox* (1972), *Hoffman*

Email addresses: `busse@uni-bayreuth.de` (F. H. Busse),
`r.simitev@maths.gla.ac.uk` (R. D. Simitev).

(1981), see also *Merrill et al.* (1996) and later papers by *Gubbins* (1999) and *Wicht* (2005)) that global excursions are aborted reversals. Not all recorded excursions are global ones, but global excursions still appear to occur more frequently than reversals. *Langereis et al.* (1997) identified at least six global excursions in the last about 800 ky since the Brunhes/Matuyama reversal, but in the last decade many more global excursions have been found according to *Lund et al.* (2006). In this letter we wish to support the notion that global excursions and reversals originate from the same mechanism. An oscillatory dynamo process that manifests itself primarily in the toroidal component of the magnetic field will be proposed as such a mechanism. Indeed, from the perspective of the oscillations, excursions must be considered as the normal behavior, while a reversal represents an exceptional excursion in which the mean poloidal field is perturbed more strongly that it can recover from its low-amplitude state only with the opposite sign.

Traditionally the geodynamo is regarded as a stationary dynamo in contrast to the solar dynamo which exhibits a 22-year period. Dynamo simulations have shown, however, that in rapidly rotating spherical fluid shells with significant differential rotation often oscillatory dynamos are found. That dynamo oscillations may not be visible from the exterior of the conducting fluid sphere has been pointed out previously (*Busse & Simitev* (2006)). The present letter intends to demonstrate how oscillations can lead to global excursions and more rarely to reversals. While the simulations are based on the fundamental equations governing the generation of magnetic fields by convection flows in rotating spherical shells, only a minimum of physical parameters is introduced and a faithful modeling of the Earth's core has not been the primary goal.

2 Mathematical formulation

We consider a spherical fluid shell of thickness d rotating with a constant angular velocity Ω. It is assumed that a static state exists with the temperature distribution $T_S = T_0 - \beta d^2 r^2 / 2$. Here rd is the length of the position vector, $\boldsymbol{r}$, with respect to the center of the sphere. The gravity field is $\boldsymbol{g} = -d\gamma\boldsymbol{r}$. In addition to the length d, the time d^2/ν, the temperature $\nu^2/\gamma\alpha d^4$ and the magnetic flux density $\nu(\mu\varrho)^{1/2}/d$ are used as scales for the dimensionless description of the problem where ν denotes the kinematic viscosity of the fluid, κ its thermal diffusivity, ϱ its density, α its coefficient of thermal expansion and μ is its magnetic permeability. The Boussinesq approximation is assumed. Accordingly, the velocity field $\boldsymbol{u}$ as well as the magnetic flux density $\boldsymbol{B}$ are solenoidal vector fields for which the general representation in terms of poloidal and toroidal components can be used,

$$\boldsymbol{u} = \nabla \times (\nabla v \times \boldsymbol{r}) + \nabla w \times \boldsymbol{r} \ , \tag{1a}$$

$$\boldsymbol{B} = \nabla \times (\nabla h \times \boldsymbol{r}) + \nabla g \times \boldsymbol{r} \ . \tag{1b}$$

2

By multiplying the (curl)^2 and the curl of the equation of motion and of the induction equation by $\boldsymbol{r}$, we obtain four equations for v and w and for h and g. These four equations together with the heat equation for the dimensionless deviation Θ from the static temperature distribution and with the appropriate boundary conditions represent the basis for the mathematical description of the evolution in time of thermal convection in the rotating spherical shell and of the magnetic field generated by it. Since these equations have been given in previous papers (*Simitev & Busse* (2005), *Busse & Simitev* (2006)), we list here only the dimensionless parameters, the Rayleigh number R, the Coriolis number τ, the Prandtl number P and the magnetic Prandtl number P_m,

$$R = \frac{\alpha\gamma\beta d^6}{\nu\kappa}, \quad \tau = \frac{2\Omega d^2}{\nu}, \quad P = \frac{\nu}{\kappa}, \quad P_m = \frac{\nu}{\lambda}, \tag{2}$$

where λ is the magnetic diffusivity. We assume stress-free boundaries with fixed temperatures and use the radius ratio $r_i/r_o = 0.4$,

$$v = \partial^2_{rr} v = \partial_r(w/r) = \Theta = 0$$
$$\text{at } r = r_i \equiv 2/3 \text{ and } r = r_o \equiv 5/3. \tag{3}$$

For the magnetic field an electrically insulating outer boundary is assumed such that the poloidal function h must be matched to the function $h^{(e)}$ which describes the potential field outside the fluid shell

$$g = h - h^{(e)} = \partial_r(h - h^{(e)}) = 0 \text{ at } r = r_o \equiv 5/3. \tag{4}$$

In order to avoid the computation of h and g in the inner core, $r \leq r_i$, we assume either an electrically insulating inner boundary,

$$g = h - h^{(e)} = \partial_r(h - h^{(e)}) = 0 \text{ at } r = r_i \equiv 2/3, \tag{5}$$

or a perfectly conducting inner core in which case the conditions

$$h = \partial_r(rg) = 0 \qquad \text{at } r = r_i \equiv 2/3 \tag{6}$$

must be applied. The numerical integration of the equations for v, w, Θ, h and g together with boundary conditions (3), (4) and (5) or (6) proceeds with the pseudo-spectral method as described by *Tilgner* (1999) which is based on an expansion of all dependent variables in spherical harmonics for the θ, φ-dependences, i.e. $$h = \sum_{l,m} H_l^m(r, t) P_l^m(\cos\theta) \exp\{im\varphi\} \tag{7}$$

and analogous expressions for the other variables, v, w, Θ and g. P_l^m denotes the associated Legendre functions. For the r-dependence expansions in Chebychev polynomials are used. Azimuthally averaged components of the fields v, w, Θ, h and g will be indicated by an overbar. For most computations to be reported here a minimum of 33 collocation points in the radial direction and spherical harmonics up to the order 96 have been used. But this high resolution was not needed in all cases. Instead of the time t based on the viscous time scale we shall use in the following the time $t^* = t/P_m$ based on the magnetic diffusion time, d^2/λ.

3 Oscillations of the Toroidal Magnetic Flux

Even in their turbulent state of motion, convection flows outside the tangent cylinder which touches the inner core boundary at its equator remain essentially symmetric with respect to equatorial plane as is evident from figure 1. For this reason dynamo solutions characterized by an axial dipole correspond to a mean azimuthal magnetic flux that is antisymmetric with respect to the equatorial plane. Oscillations of these axisymmetric flux tubes originate from the creation of a pair of new flux tubes with opposite signs at the equatorial plane which grow and push the older flux towards higher latitudes as shown in figure 2. This process is strongly dependent on the differential rotation which is prograde at larger distances from the axis and retrograde at smaller ones. The oscillations can be described by Parker's dynamo wave model (*Parker* (1955)) as has been done by *Busse & Simitev* (2006). In the present case of figure 2 the oscillation is modified in two respects. First, the mean toroidal field becomes nearly quadrupolar, i.e. symmetric about the equatorial plane, as the amplitudes of the mean poloidal field and of the differential rotation reach their minimum values. Secondly and more importantly, the mean poloidal field participates in the oscillation only as far as its amplitude varies. In the case of figure 2 its amplitude decays and reaches a minimum around $t^* \approx 1.6$ at which time a magnetic eddy emerges with the opposite sign of the given mean poloidal field. Usually this eddy drifts outward and dissipates as it reaches the surface of the conducting region such that the original poloidal field prevails. Now a relatively long time passes before the process repeats itself and new toroidal flux emerges at the equatorial plane. In contrast to the thinner flux tubes of dynamos at higher Prandtl numbers which exhibit a more sinusoidal oscillation as shown in section (b) of figure 3, the oscillation in the present case resembles more a relaxation oscillation as shown in section (a) of figure 3. The amplitudes H_l^0, G_l^0 in this figure are assumed at the mid-radius of the fluid shell, but H_1^0 usually does not differ much from the dipole component describing the magnetic field outside the fluid shell.

While the process visualized in figure 2 shares several features with global excursions, it may also give rise to reversals. These happen in some cases when the emerging eddy with the opposite sign of the poloidal field replaces the latter as shown in figure 4. This situation occurs most likely if the eddy with the opposite sign emerges near the equatorial plane such that it splits the original field into two parts. It is remarkable that the reversed poloidal field appears first at low latitudes as has also been observed in the case of geomagnetic reversals (*Clement* (2004)). Note that the radius $r = r_o + 1.3$ corresponds approximately to the Earth's surface. The occurrence of a reversal seems to be promoted by a particularly strong equatorially symmetric toroidal flux as appears to be indicated by the correlation between reversals and relative high absolute values of the coefficient G_1^0 in sections (b) and (c) of figure 3. We

note in passing that Li et al. (2002), propose a reversal mechanism in which the quadrupole mode grows, exceeding the dipole mode before the reversal in a manner similar to what happens near the minimum of the oscillations shown in figure 2. In contrast, however, our dynamo solutions do not alternate between high- and low-energy states, nor do they exhibit a broken columnar vortex structure of the velocity field.

The examples discussed so far all correspond to a single set of parameter values. In particular condition (6) for a highly electrically conducting core has been used. In order to demonstrate the robust nature of the mechanism of global excursions and reversals, we show in figure 5 a sequence of plots exhibiting a reversal from a dynamo simulation with a quite different set of parameters for which condition (5) instead of (6) has been applied. The oscillations occur somewhat less regularly in this case as is evident from the time series of the amplitude of the axial dipole component shown in section (c) of figure 3, but the average period is again close to half a magnetic diffusion time. A common property of the oscillations is that the quadrupolar components of the axisymmetric magnetic field play a significant role. In this respect some similarity may be noted with the oscillations displayed in figures 12 and 13 of *Busse & Simitev* (2006).

Although the inner core does not participate in the oscillations in either of the boundary conditions (5) and (6), we expect that the use of a vanishing jump of the electrical conductivity at $r = r_i$ will not affect the results significantly. As has been observed in the dynamo simulations of *Wicht* (2002) and of *Simitev & Busse* (2005), because of its small volume the inner core does not appear to have a significant effect on the dynamo process.

4   Discussion

In selecting the dynamo cases displayed in figures 2, 4 and 5 we have emphasized a high value of τ and a reasonably high value of R for which the available computer capacity allows to obtain time records extending over many magnetic diffusion times. The critical values of the Rayleigh numbers for $\tau = 3 \times 10^4$ and $\tau = 10^5$ are $R_c = 2.35 \times 10^4$ with $m_c = 10$ and $R_c = 1.05 \times 10^6$ with $m_c = 11$, respectively. Hence the Rayleigh numbers used for the cases of figures 2, 4 and 5 exceed their critical values by nearly a factor of four. The corresponding average Nusselt numbers at the inner boundary are $Nu_i = 1.58$ and $Nu_i = 1.73$ and the corresponding magnetic Reynolds numbers, defined by $R_m \equiv P_m \sqrt{2E}$, are $R_m = 210$ and $R_m = 156$, respectively. The Prandtl number $P = 0.1$ was used in both cases since it appears to be a reasonable compromise between the molecular value $P = 0.05$ estimated for the outer core (*Poirier* (1988)) and a value of the order unity usually assumed for a highly turbulent fluid. Moreover, the choice of a low value of P has allowed

5

us to choose a desirable relatively low value of P_m.

The successful application of Parker's kinematic model for dynamo waves employed by *Busse & Simitev* (2006) suggests that the oscillations depend primarily on the differential rotation and the mean helicity of convection which are assumed as given. The modified oscillation considered in the present paper is characterized by an extended phase of a dominant equatorially symmetric (quadrupolar) mean toroidal field which is responsible for the property that the period becomes comparable to the magnetic diffusion time. The variations of the amplitude of convection and of the differential rotation seem to be of lesser importance.

Using the depth $d \approx 2200$ km of the liquid outer core and a typical and often quoted value $\lambda \approx 2$ m^2/s we find 0.8×10^5 years as the magnetic diffusion time of the Earth's core which corresponds to $t^* = 1$ in the figures of this paper. The oscillation period $T^* \approx 0.5$ obtained in the time series of figure 3(a) thus roughly equals about 40 ky in the Earth's core. This period is quite comparable to the broad maximum in the region of 30-50 ky that seems to characterize the spectrum of the amplitude variations of the geomagnetic field (*Tauxe & Shackleton* (1994), *Tauxe & Hartl* (1997), *Guyodo & Valet* (1999)) throughout the last million years. A more recent analysis (*Constable & Johnson* (2005)) has shed some doubts on the existence of such a spectral peak, but still confirms a sharp decrease of the spectral power for periods shorter than about 30 ky. We also like to draw attention to the property that the typical separation between global excursions in table 1 of *Lund et al.* (2006) varies between 30 and 50 ky.

From the reversals exhibited in figures 3, 4 and 5 it appears that the amplitude increases more sharply after the reversal than it decays towards the reversal. To demonstrate this effect more clearly we have plotted in figure 6 the coefficient H_1^0 in proximity of the reversal as a function of time for each of the last 4 reversals that have been obtained in the cases a) and c) of figure 3. Although the asymmetry between the dipole strengths before and after the reversal is not as strong as has been found in the case of paleomagnetic reversals (*Valet et al.* (2005), *Guyodo & Valet* (2006)), a similar effect seems to exist. Since the time records of figure 3 do not exhibit this effect very well we have plotted in figure 6 values of H_1^0 at $r = r_i + 0.5$ for shorter time periods. In the case $R = 850000$ H_1^0 at $r = r_o$ is also shown (by solid lines) since it represents the axial dipole strength of the potential field outside the fluid shell. Apart from a small shift in time the value of H_1^0 does not vary much as function of the radius. In the continuing investigation of the dynamo oscillations it will be attempted to find even closer correspondences with paleomagnetic observations.

The possibility of toroidal flux oscillations as origin of global excursions and reversals proposed in this paper differs from all other mechanisms proposed

in the literature for reversals and excursions and resembles more the mechanisms considered for the solar cycle. In the latter the mean poloidal field fully participates, of course, similarly as in the dipole oscillation of figure 10 of *Busse & Simitev* (2006) except for the property that the solar dynamo wave propagates towards lower instead of higher latitudes. A comparison of different mechanisms for geomagnetic reversals would go beyond the scope of present paper and should be postponed until more detailed computational results for a wider range of parameters become available.

References

Busse, F.H., and Simitev, R., Parameter dependences of convection-driven dyanamos in rotating spherical fluid shells, *Geophys. Astrophys. Fluid Dyn. 100,* 341-361, 2006.

Clement, B. M. Dependence of the duration of geomagnetic polarity reversals on site latitude, *Nature 428,* 637-640, 2004.

Constable, C., and Johnson, C., A paleomagnetic power spectrum, *Phys. Earth Plan. Int. 153,* 61-73, 2005.

Doell, R.R., and Cox, A.V., The Pacific geomagnetic secular variation anomaly and the question of lateral uniformity in the lower mantle. *in The Nature of the Solid Earth, E. C. Robertson, ed., McGraw-Hill, New-York, p. 245,* 1972.

Guyodo, Y., and Valet, J.-P., Global changes in intensity of the Earth's magnetic field during the past 800 kyr, *Nature 399*, 249-252, 1999.

Guyodo, Y., and Valet, J.-P., A comparison of relative paleointensity records of the Matuyama Chron for the period 0.75-1.25 Ma, *Phys. Earth Plan. Int. 156*, 205-212, 2006.

Gubbins, D., The distinction between geomagnetic excursions and reversals, *Geophy. J. Int. 137,* F1-F3, 1999.

Hoffman, K.A., Paleomagnetic excursions, aborted reversals and transitional fields, *Nature 294,* 67, 1981.

Langereis, C.G., Dekkers, M.J., de Lange, G.J., Paterne, M. and van Santwort, P.J.M., Magnetostratigraphy and astronomical calibrations of the last 1.1 Myr from an eastern Mediterranean piston core and dating of short events in the Brunhes, *Geophy. J. Int. 129,* 75-94, 1997.

Li, J., Sato, T. and Kageyama, A., Repeated and sudden reversals of the dipole field generated by a spherical dynamo action , *Science 5561,* 1887-1890, 2002.

Lund, S., Stoner, J. S., Channell, J.E.T., Acton, G., A summary of Brunhes paleomagnetic field variability recorded in Ocean Drilling Program cores, *Phys. Earth Plan. Int. 156,* 194-205, 2006.

Merrill, R.T., McElhinny, M.W., & McFadden, P.L., *in The Magnetic Field of the Earth, Academic Press, San Diego*, 1996.

Parker, E. N., Hydromagnetic dynamo models. *Astrophys. J. 121* 293-314, 1955.

Poirier, J.-P., Transport properties of liquid metals and viscosity of the Earth's core, *Geophy. J. Int. 92*, 99-105, 1988.

Simitev, R. and Busse, F.H. 2005 Prandtl-number dependence of convection-driven dynamos in rotating spherical fluid shells. *J. Fluid Mech. 532*, 365-388.

Tauxe, L., and Hartl, P., 11 million years of Oligocene geomagnetic field behavior, *Geophy. J. Int. 128,* 217-229, 1997.

Tauxe, L., and Shackleton, N.J., Relative paleointensity records from the Ontong-Java Plateau, *Geophy. J. Int. 117,* 769-782, 1994.

Tilgner, A., Spectral Methods for the Simulation of Incompressible Flows in Spherical Shells. *Int. J. Numer. Meth. Fluids, 30,* 713-724, 1999.

Valet, J.-P., Meynardier, L., and Guyodo, Y., Geomagnetic dipole strength and reversal rate over the past two million years, *Nature 435,* 802-805, 2005.

Wicht, J., Inner core conductivity in numerical dynamo simulations, *Phys. Earth Planet. Inter. 132,* 281-302, 2002.

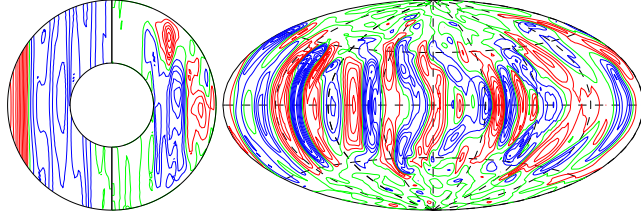Wicht, J., Paleomagnetic interpretations of dynamo simulations, *Geophy. J. Int. 162,* 371-380, 2005.

Fig. 1. (color online). Typical structures of the velocity field in the case $P = 0.1$, $\tau = 10^5$, $R = 4 \times 10^6$, $P_m = 0.5$ with a perfectly electrically conducting inner core. The left plot shows lines of constant $\overline{u}_\varphi$ in the left half and streamlines $r \sin \theta \partial_\theta \overline{v} =$const. in the right half, all in the meridional plane. The right plot shows lines of constant u_r at $r = r_i + 0.5$ at the time $t^* = 1.486$. Positive and negative values are indicated by solid (red online) and dashed (blue online) lines.
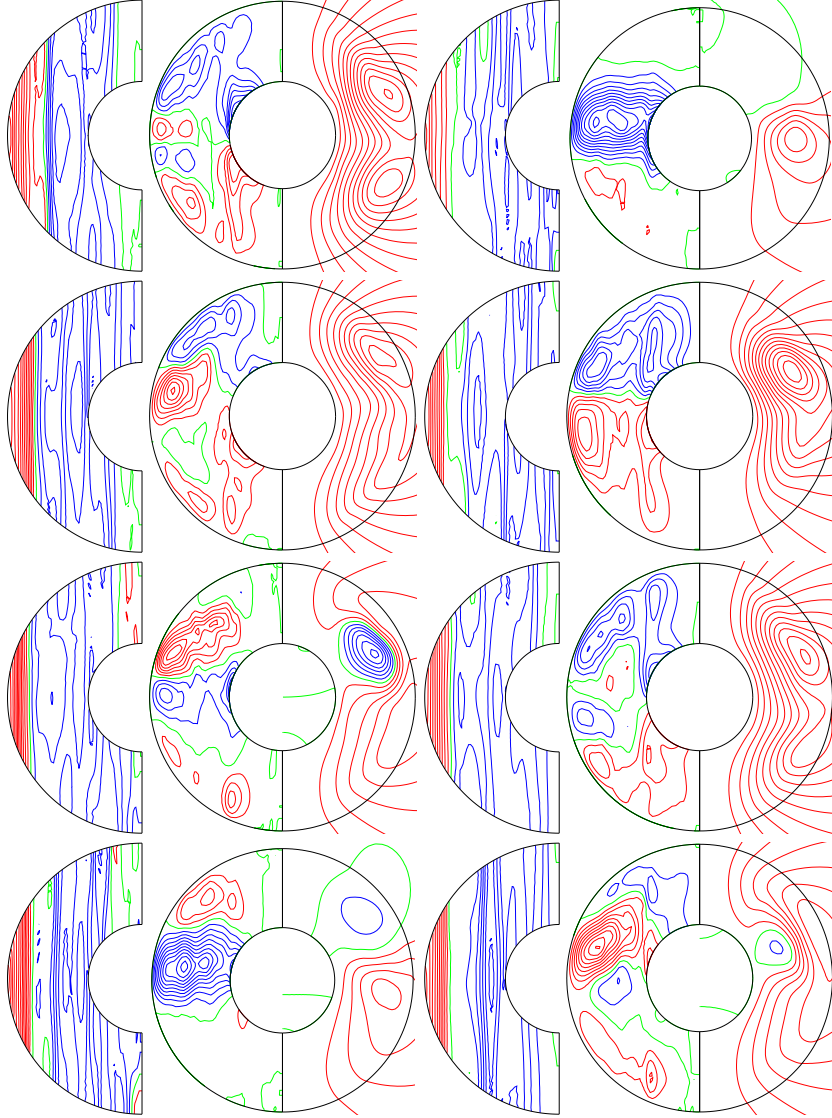
Fig. 2. (color online). Dynamo oscillation in the case $P = 0.1$, $\tau = 10^5$, $R = 4 \times 10^6$, $P_m = 0.5$ with perfectly conducting inner core. The half circles show lines of constant $\overline{u}_\varphi$. The full circles show meridional isolines of $\overline{B}_\varphi$ (left half) and of $r \sin \theta \partial_\theta \overline{h}$ (right half) at times $t^* = 1.490$, 1.538, 1.586, 1.634, (first column, from top to bottom) and $t^* = 1.682$, 1.810, 1.954, 2.034 (second column). The times t^* refer to figure 3(a).
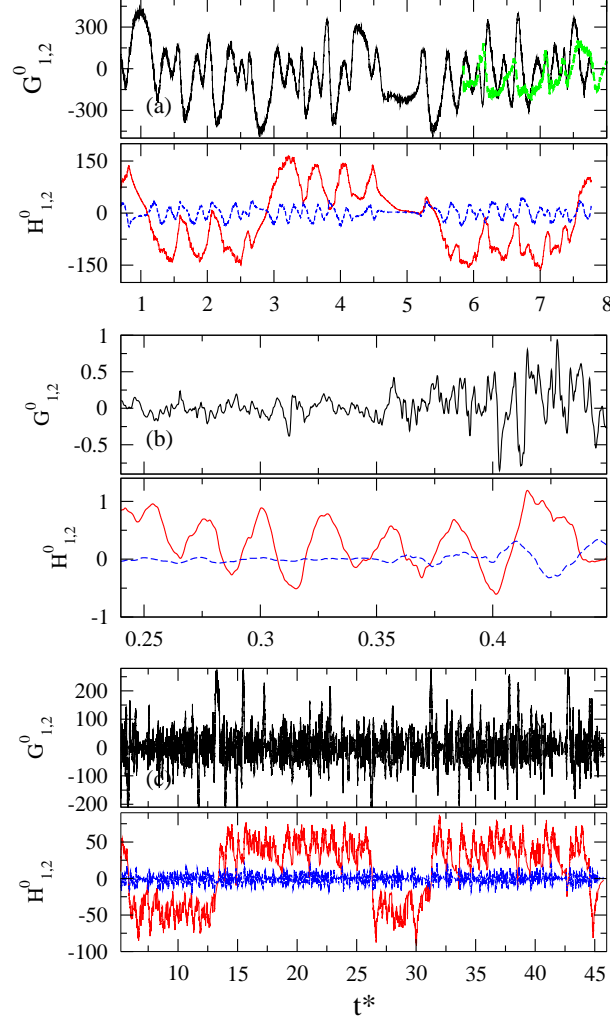
Fig. 3. (color online). Selected coefficients at $r = r_i + 0.5$ in the cases (a) $P = 0.1$, $\tau = 10^5$, $R = 4 \times 10^6$, $P_m = 0.5$ with perfectly conducting inner core; (b) $P = 5$, $\tau = 5000$, $R = 600000$, $P_m = 10$ with electrically insulating inner core; (c) $P = 0.1$, $\tau = 3 \times 10^4$, $R = 850000$, $P_m = 1$ with insulating inner core. The coefficient of the axial dipole component H_1^0 (axial quadrupole component H_2^0) is indicated by a solid/red online (dashed/blue online) line. The coefficient G_2^0 in (a) is indicated by a dashed/green online line.
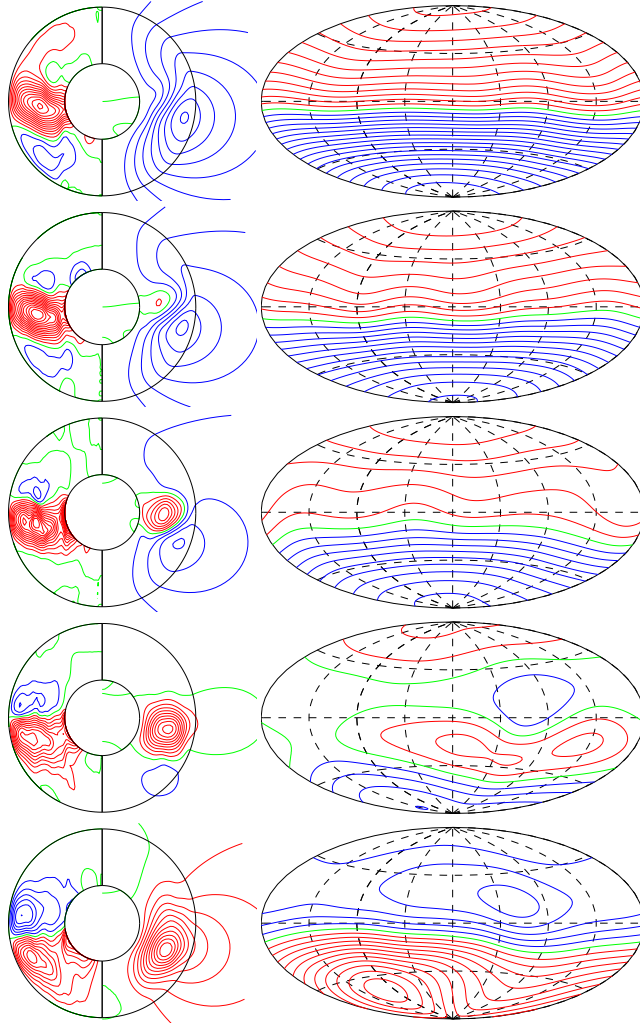
Fig. 4. (color online). Magnetic field polarity reversal in the case $P = 0.1$, $\tau = 10^5$, $R = 4 \times 10^6$, $P_m = 0.5$ with perfectly conducting inner core. The left column shows meridional isolines of $\overline{B}_\varphi$ (left half) and of $r \sin\theta \partial_\theta \overline{h}$ (right half). The right column shows lines $B_r = $ const. at $r = r_o + 1.3$. The interval between the plots is $\Delta t^* = 0.048$ with the first plot at $t^* = 0.994$ (see figure 3(a)).
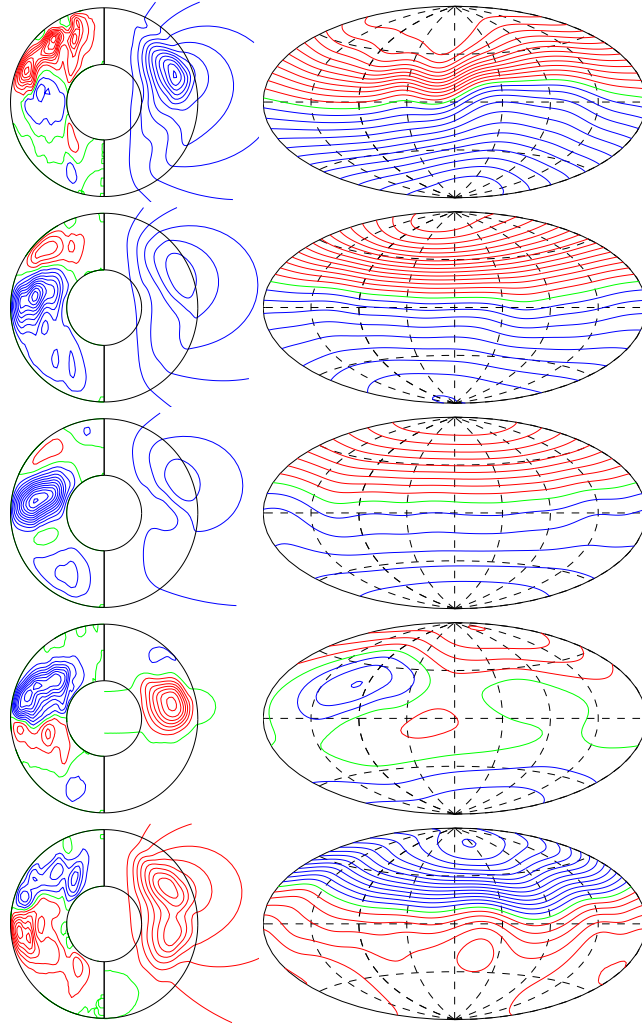
Fig. 5. (color online). Same as figure 4, but for $P = 0.1$, $\tau = 3 \times 10^4$, $R = 850000$, $P_m = 1$ with insulating inner core. The interval between the plots is $\Delta t^* = 0.07$ with the first plot at $t^* = 26.155$ (see figure 3(c)).
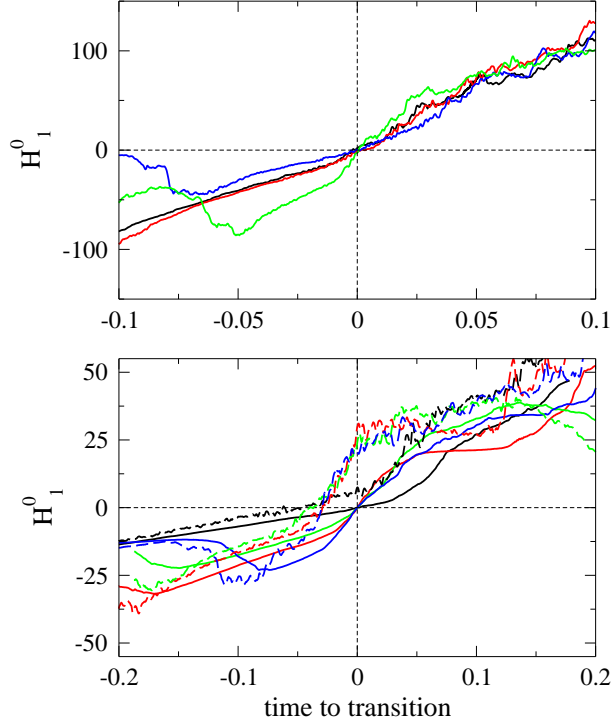
Fig. 6. (color online). Time-series of the coefficients of the axial dipole component H_1^0 at $r = r_i + 0.5$ across the last 4 reversals in the cases $P = 0.1$, $\tau = 10^5$, $R = 4 \times 10^6$, $P_m = 0.5$ with perfectly conducting inner core (top) and $P = 0.1$, $\tau = 3 \times 10^4$, $R = 850000$, $P_m = 1$ with insulating inner core (bottom). For the sake of comparison, the time series have been translated along the time axis so that the polarity transitions occur at $t = 0$ and $-H_1^0$ is plotted for every second reversal. In both panels, black, red, blue and green color correspond to reversals 1(2) to 4(5) of the respective cases in figure 3. In the bottom panel, H_1^0 at $r = r_o$ has been included in order to represent the axial dipole strength of the potential field outside the fluid shell. H_1^0 at $r = r_i + 0.5$ (given by dashed lines) precedes it by about $\Delta t^* \approx 0.04$

14